Gradient-Enhancing Conversion for Illumination-Robust Lane Detection

Hunjae Yoo, Ukil Yang, and Kwanghoon Sohn, *Senior Member, IEEE*

***Abstract*—Lane detection is important in many advanced driver-assistance systems (ADAS). Vision-based lane detection algorithms are widely used and generally use gradient information as a lane feature. However, gradient values between lanes and roads vary with illumination change, which degrades the performance of lane detection systems. In this paper, we propose a gradient-enhancing conversion method for illumination-robust lane detection. Our proposed gradient-enhancing conversion method produces a new gray-level image from an RGB color image based on linear discriminant analysis. The converted images have large gradients at lane boundaries. To deal with illumination changes, the gray-level conversion vector is dynamically updated. In addition, we propose a novel lane detection algorithm, which uses the proposed conversion method, adaptive Canny edge detector, Hough transform, and curve model fitting method. We performed several experiments in various illumination environments and confirmed that the gradient is maximized at lane boundaries on the road. The detection rate of the proposed lane detection algorithm averages 96% and is greater than 93% in very poor environments.**

***Index Terms*—Gradient-enhancing conversion, illumination-robust method, lane detection, linear discriminant analysis (LDA).**

I. Introduction

With the increase in the number of vehicles, the number of car accident victims has increased annually. Many accidents are caused by a lack of awareness about driving conditions due to driver carelessness or visual interference. Advanced driver-assistance systems (ADAS) are regarded as an important technology to reduce such accidents.

Lane detection and tracking are considered as a basic module for ADAS. These algorithms are the core of lane departure warning systems and lane keeping systems. In addition, information about the detected lane position can be used to detect approaching vehicles and obstacles.

Almost all lane detection algorithms use the following three steps: lane feature extraction, outlier removal, and tracking [1]. Feature extraction is an important step in lane detection. If the feature is not correctly detected, it is difficult to compensate during postprocessing. Many features such as colors [2], corners, edges [3]–[6], and geometric shapes [7] can be used to represent lanes. Edges are one of the most significant features because lanes create strong edges on the road. In other words, large gradients exist between the road and the lane due to the difference in their intensities. Thus, many conventional methods use gradient-based features.

These gradient-based lane detection algorithms apply gradient feature extraction to a gray-level image obtained from a certain ratio of RGB or luminance coefficients in YCbCr. However, they have a problem in detecting lane features, which have large gradients compared with the road. Since color lanes are transformed into a gray value similar to the road, gradients between color lanes and the road are highly depressed and may cause lane detection failure. This can cause critical problems in real applications because color lanes may convey more important information, such as centerlines.

Sun *et al.* [8] used a saturation image to compensate for the weakness of the gray-level image. Cheng *et al.* [9] proposed a new color space whose channels represent the RGB color difference. They also analyzed the color distribution of roads and lanes in their proposed color space and extracted the land marking color with the Gaussian-distributed assumption. Several approaches have been proposed. Wang *et al.* [10] used histogram equalization, which gives greater contrast to an image to compensate gradient depression. Kim [6] empirically determined RGB weights, which makes larger gradients between lanes and roads. However, illumination can vary with time, weather, and light in outdoor road environments. Therefore, a fixed RGB ratio or off-line color analysis in the previous approaches cannot control all those conditions. A dynamic brightness compensation method was proposed in [11], which applies gamma correction to conventional gray-level images. The gamma correction coefficients are generated from analysis of the cumulative value of pixels based on the self-clustering algorithm (SCA) and fuzzy C-mean. When roads and lanes produce separate clusters, it works well. However, the intensity values of roads and lanes are often classified into the same cluster. Thus, the fundamental problem of the color lane and road being converted into similar values is not resolved.

In this paper, we propose a linear discriminant analysis (LDA)-based gradient-enhancing conversion for illumination-robust lane detection. Our method generates optimal RGB weights that maximize gradients at lane boundaries on the road to distinguish lanes from roads. This paper is structured as follows: Section II describes problems of the conventional gray-level image conversion method. Section III proposes a

Manuscript received December 23, 2011; revised July 30, 2012; accepted February 27, 2013. This work was supported by a grant from the R&D Program (Industrial Strategic Technology Development) funded by the Ministry of Knowledge Economy (MKE), Republic of Korea. The authors acknowledge all interested persons of MKE and the Korea Evaluation Institute of Industrial Technolgy (KEIT) (10040018, Development of 3D Montage Creation and Age-specific Facial Prediction system). The Associate Editor for this paper was Q. Ji.

The authors are with the School of Electrical and Electronic Engineering, Yonsei University, Seoul 120-749, Korea (e-mail: gnswo0112@yonsei.ac.kr; starb612@yonsei.ac.kr; khsohn@yonsei.ac.kr).

Color versions of one or more of the figures in this paper are available online at http://ieeexplore.ieee.org.

Digital Object Identifier 10.1109/TITS.2013.2252427

Fig. 1. Example of a color image in a driving environment.

gradient-enhancing conversion method for illumination-robust lane detection. Section IV describes some experimental results under various illumination conditions to confirm the excellence of the proposed algorithm. Finally, Section V discusses our conclusion and future works.

II. Revisit to Existing Gradient-Enhancing Methods for Lane Detection Algorithms

Edges, ridges, or steerable filters are used as lane features in many lane detection algorithms and are based on gradient information in a gray-level image [12]. Gradient-based lane features are usually used for lane detection under the assumption that gray-level values of lanes and roads significantly differ. In certain illumination conditions, however, the difference is not sufficiently large since lanes and roads are converted into similar gray-level values. That is, the gradients between lanes and roads are too small to adequately extract lane features. In this paper, we refer to the gradients between lanes and roads as lane gradients, for convenience.

Here, we introduce conventional gray-level image conversion methods and their problems. In addition, we present several existing methods to overcome the problem and show that they still have some limitations in lane detection in various environments.

A. Conventional Gray-Level Image Conversion Method

Many lane detection algorithms [13]–[16] based on gradient features do not consider the problems of conventional gray-level image conversion methods. Conventional methods use an averaging RGB channel or luminance channel in color space such as YCbCr. The YCbCr conversion matrix is shown in the following equation as an example:

$$\begin{bmatrix} Y \\ Cb \\ Cr \end{bmatrix} = \begin{bmatrix} 0.299 & 0.587 & 0.114 \\ -0.169 & -0.331 & 0.500 \\ 0.500 & -0.419 & 0.081 \end{bmatrix} \begin{bmatrix} R \\ G \\ B \end{bmatrix} + \begin{bmatrix} 0 \\ 128 \\ 128 \end{bmatrix} \quad (1)$$

where Y is the luminance channel, and Cb and Cr represent the blue and red differences, respectively.

Fig. 2 shows examples of gray-level images for the color image in Fig. 1 after being converted by a conventional method. While lanes and roads are clearly distinguished in color images, they are similar to the converted images, as shown in Fig. 2.

(a) (b)

Fig. 2. Gray images for Fig. 1 obtained by conventional methods. (a) Average of RGB. (b) Y channel in YCbCr.

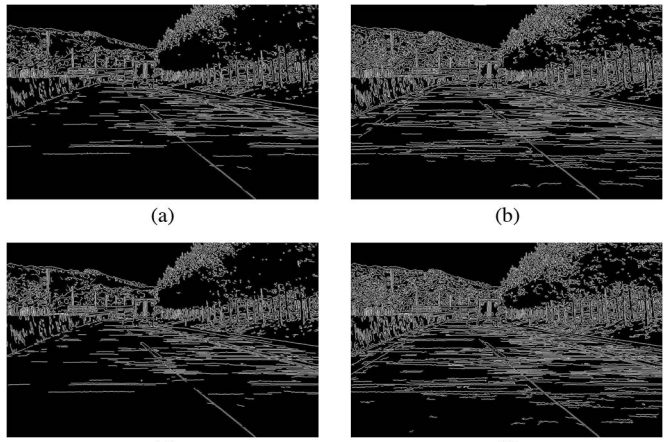

(a) (b) (c) (d)

Fig. 3. Canny edge detection results with different thresholds. (a) $th_s = 60$, $th_l = 100$ to Fig. 2(a). (b) $th_s = 30$, $th_l = 50$ to Fig. 2(a). (c) $th_s = 60$, $th_l = 100$ to Fig. 2(b). (d) $th_s = 30$, $th_l = 50$ to Fig. 2(b).

(a) (b)

Fig. 4. Gradient-enhancing results of conventional methods. (a) Histogram equalization. (b) Fixed RGB ratio (0.5 for red, 0.4 for green, and 0.1 for blue) [6].

It is difficult to properly extract gradient features in converted gray-level images. Fig. 3 shows the edge detection results in Fig. 2. Edges for yellow lanes are not detected, as shown in Fig. 3(a) and (c). If we use a smaller threshold value, the lane edges may be detected. However, too many unwanted edges are also detected, as shown in Fig. 3(b) and (d). We may need a complex outlier removal process to overcome this problem.

B. Contrast-Enhancing Methods Based on a Histogram

Intuitively, white lanes have high intensity values, and roads have low intensity values. Histogram equalization, which is an algorithm for contrast adjustment, can be used to enhance gradients between white lanes and roads. However, the intensity of the yellow lane is similar to that of the road in many situations. In other words, the histogram-based method does not work well if the road and the lane have similar intensity values, as shown in Fig. 4(a) [17], [18].

C. Modified RGB Ratio-Based Gradient-Enhancing Conversion Method

In [6], classification performance with a neural network was simulated for color and gray-level images with two different ratios. Gray-level images converted by their ratio (0.5 for red, 0.4 for green, and 0.1 for blue) are better than those of equal-weight conversion for detecting yellow lane markings, as shown in Fig. 4(b). This observation may be reasonable under daylight conditions since both yellow and white lanes have higher values than the road in the red and green channel. However, the problem remains under different color temperature illuminations, such as evening sun or artificial lighting conditions.

D. Brightness Compensation Method Based on Gray-Level Clustering

Wang *et al.* [11] proposed a lane detection algorithm to address illumination problems caused by weather conditions. They performed brightness compensation in the Y channel image of the YIQ color space, where I stands for in-phase, and Q stands for quadrature. They analyzed the histogram of the Y channel image and divided the Y channel image into light and dark components by an SCA and fuzzy C-mean clustering. For each component, compensation is achieved based on the gamma correction shown in (2). The correction term, i.e., α from (2), is calculated by the fuzzy logic membership function. Thus

$$c(i) = (p(i)/255)^{\alpha} \times 255 \tag{2}$$

where $c(i)$ is the compensated intensity at the ith pixel, and $p(i)$ is the original intensity at the ith pixel. The method of Wang *et al.* analyzes the frame and applies an adaptive correction process to the frame. If roads and lanes are classified as different clusters, the gradient is adequately enhanced. If classification fails, brightness is not well compensated. Misclassification may occur because lanes and roads have similar intensity values in many situations.

All approaches based on gray-level image enhancement (such as contrast enhancement and brightness compensation) have limitations. If the original gray levels are similar, then the enhanced values are also similar. Thus, the information that is lost by the gray-level image conversion process cannot be recovered. In addition, the modified RGB ratio-based method does not guarantee that gradients between lanes and roads remain appropriate under various illumination conditions. Therefore, a new conversion method is needed to produce larger gradients between lanes and roads in various illumination conditions to properly detect lanes.

III. Proposed Method

Here, we propose a gradient-enhancing conversion method that produces a lane-gradient-maximized image from a color image. In addition, we propose an illumination-robust lane detection algorithm based on the gradient-enhancing conversion method.

A. Gradient-Enhancing Conversion

The color image acquisition process is modeled as follows [19]:

$$\begin{bmatrix} R_i \\ G_i \\ B_i \end{bmatrix} = \begin{bmatrix} \int E(\lambda) S_i(\lambda) Q_R(\lambda) d\lambda \\ \int E(\lambda) S_i(\lambda) Q_G(\lambda) d\lambda \\ \int E(\lambda) S_i(\lambda) Q_B(\lambda) d\lambda \end{bmatrix} \tag{3}$$

where λ denotes the wavelength of light; R_i, G_i, and B_i are the RGB values of the ith pixel of the image; $E(\lambda)$ denotes the spectral power distribution of light; and $S_i(\lambda)$ is the object surface reflectance for the ith pixel. The spectral sensitivities of the RGB sensors are denoted by $Q_R(\lambda)$, $Q_G(\lambda)$, and $Q_B(\lambda)$, respectively. In other words, $E(\lambda)$ is determined by illumination conditions, $S_i(\lambda)$ is determined by the object surface color, and $Q(\lambda)$ is determined by the characteristics of the camera sensor. Thus, RGB values of an image of the same color object captured by the same camera can vary with illumination changes. This means that the fixed-RGB-ratio method cannot produce the best solution to solve the lane-gradient maximization problem in various illumination conditions.

To address the given problem, we dynamically generate a conversion vector that can be adapted in various illumination and road conditions. The conversion vector converts a color image into a gray-level image to provide the maximum lane gradient. The conversion vector is updated by the lane and road color information of the previous frames.

Gray-level conversion is generally performed by the weighted sum of RGB as follows:

$$y = w_R R + w_G G + w_B B \tag{4}$$

where w_R, w_G, and w_B are weights of RGB, and y is a conversion value of (R, G, B). The lane gradient in the converted image is mathematically represented as follows:

$$g_l = \nabla(y_r, y_l) = |y_r - y_l| \tag{5}$$

where y_r and y_l are gray-level values of roads and lanes, respectively.

Equation (4) can be represented as the inner product between a conversion vector and an RGB vector. Thus, we represent a conversion value of the ith pixel of an image by conversion vector $\mathbf{w}$ as follows:

$$y_i(\mathbf{w}) = \mathbf{w} \cdot \mathbf{x}_i \tag{6}$$

where $\mathbf{w}$ denotes a conversion vector of RGB (w_R, w_G, w_B), and $\mathbf{x}_i$ denotes an RGB vector (R_i, G_i, B_i). The inner product is geometrically interpreted as the scalar projection of one vector onto another vector. Thus, y_i from (6) is the scalar projection of $\mathbf{x}_i$ onto weight vector $\mathbf{w}$. In other words, y_i can be achieved by dimension reduction from a 3-D vector to a 1-D scalar. Using (6), g_l from (5) can be represented as follows:

$$\begin{aligned} g_l(\mathbf{w}) &= |y_r(\mathbf{w}) - y_l(\mathbf{w})| \\ &= |\mathbf{w} \cdot \mathbf{x}^r - \mathbf{w} \cdot \mathbf{x}^l| \end{aligned} \tag{7}$$

where $\mathbf{x}^r$ and $\mathbf{x}^l$ are RGB pixel values of the road and lane regions, respectively. Therefore, gradient-enhancing conversion involves finding vector $\mathbf{w}_{\max}$ that satisfies the following equation:

$$\begin{aligned} g_l(\mathbf{w}_{\max}) &= \max\left(g_l(\mathbf{w})\right) \\ &= \max\left(\left|\mathbf{w}\cdot\mathbf{x}^r - \mathbf{w}\cdot\mathbf{x}^l\right|\right). \end{aligned} \tag{8}$$

Since gray-level image conversion in (6) is a kind of dimension reduction, (8) can be solved by finding a dimension reduction vector that results in different converted values for the road and lane classes. To obtain the dimension reduction vector $\mathbf{w}_{\max}$ of an image from (8), we should know $\mathbf{x}^r$ and $\mathbf{x}^l$ of the image, which are defined by training data. Training data consist of road and lane classes. To create training data for a current image, we need to know the RGB values of the lanes and roads in the image. However, since this is a preprocessing step for the lane detection algorithm, the information is not sufficient to extract the training data in the current frame. Thus, training data for the current frame are extracted from several previous frames. Details of the creation and updating processes for training data are explained in Section III-B.

Training data for class c for the frame at time t are defined as follows:

$$T_c^t = \left\{X_c^{t-k}, X_c^{t-(k-1)}, X_c^{t-(k-2)}, \ldots, X_c^{t-1}\right\} \tag{9}$$

where T_c^t is training data of class c for the frame at time t, c is either the lane or the road, X_c^t denotes training data for class c extracted from the frame at time t, and k is the number of previous frames to be used as training data for a current frame.

The problem in (8) becomes identification of the dimension reduction vector that maximizes discriminance between different classes and that can be solved by the LDA approach, which is a method frequently used in statistics, pattern recognition, and machine learning to find a linear combination of features that characterize or separate two or more classes of objects or events. LDA uses two different variances to find the linear combination between-class-scatter S_B and within-class-scatter S_W. Each term is defined as follows:

$$S_B = \sum_{i=1}^{c} n_i(\mathbf{m}_i - \mathbf{m})(\mathbf{m}_i - \mathbf{m})^T \tag{10}$$

$$S_W = \sum_{i=1}^{c} \sum_{\mathbf{x}\in C_i} (\mathbf{x} - \mathbf{m}_i)(\mathbf{x} - \mathbf{m}_i)^T \tag{11}$$

where $\mathbf{x}$ is data, n_i is the number of data in class i, $\mathbf{m}_i$ is the mean of class i, $\mathbf{m}$ is the mean of all data, c is the number of classes, and C_i is a set of all data in class i.

To distinguish different classes, the between-class-scatter of $\mathbf{wx}$ should be maximized, and the within-class-scatter should be minimized. Thus

$$\mathbf{w} = \arg\max \frac{|\mathbf{w}^T S_B \mathbf{w}|}{|\mathbf{w}^T S_W \mathbf{w}|}. \tag{12}$$

Lane class is divided into a yellow-lane class and a white-lane class, since lanes are generally marked with white or yellow. To maximize gradient enhancement, we identify two conversion vectors: one to enhance white-lane gradients and the other to enhance yellow-lane gradients. Thus, the two-class LDA method is used, and two converted images are generated from one color image. Fig. 5 shows an example of gradient-enhanced converted images. Fig. 5(a) is a white-lane-gradient-enhanced image, and Fig. 5(b) is a yellow-lane-gradient-enhanced image. In both images, yellow and white lanes are more noticeable than in the other methods shown in Figs. 2 and 4. Both white- and yellow-lane gradients are greater than those of the other methods, as shown in Table I.

(a)

(b)

Fig. 5. Lane-gradient-enhanced image of Fig. 1. (a) White-lane gradient. (b) Yellow-lane gradient.

B. Lane Detection Algorithm

Based on the gradient-enhancing conversion method described in the previous section, we implement an illumination-robust lane detection algorithm. The proposed algorithm starts from an image conversion based on the gradient-enhancing vector. Edge detection is then performed as a feature extraction method. The Hough transform (HT) and edge linking method are used for initial lane estimation. Final lane detection results are produced by fitting the lane model. Training data are updated to adapt illumination changes. In the update step, we extract new training data for the next frame. The overall process of the algorithm is shown in Fig. 6. Details of each step are represented as follows.

Edge detection preserves important structural properties and significantly reduces the amount of data. Among the edge detection algorithms, we use the Canny edge detector with adaptive threshold values. The Canny edge detector uses two

TABLE I
AVERAGE OF EACH CLASS AND LANE GRADIENTS OF PREVIOUS METHODS AND THE PROPOSED METHOD FOR FIG. 1

	Road	White lane	White-lane-gradient	Yellow lane	Yellow-lane-gradient
HSI	124.11	171.71	47.60	121.46	2.65
YUV	125.55	170.71	45.16	127.01	1.46
Histo eq.	198.34	230.72	32.38	202.40	4.06
Kim's method [6]	126.65	168.85	42.2	130.54	3.89
Proposed (white)	100.05	152.42	52.37	80.32	19.73
Proposed (yellow)	130.13	66.01	64.12	150.48	20.36

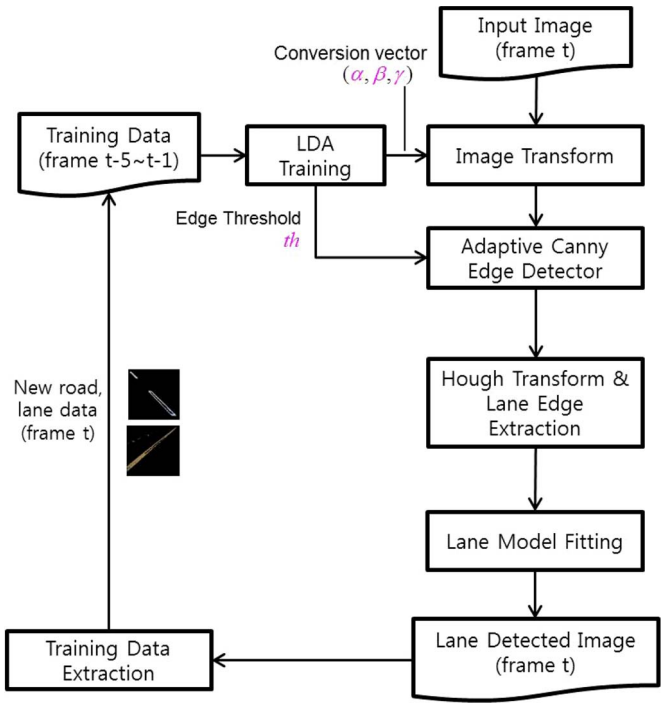

Fig. 6. Flowchart of lane detection and tracking algorithm.

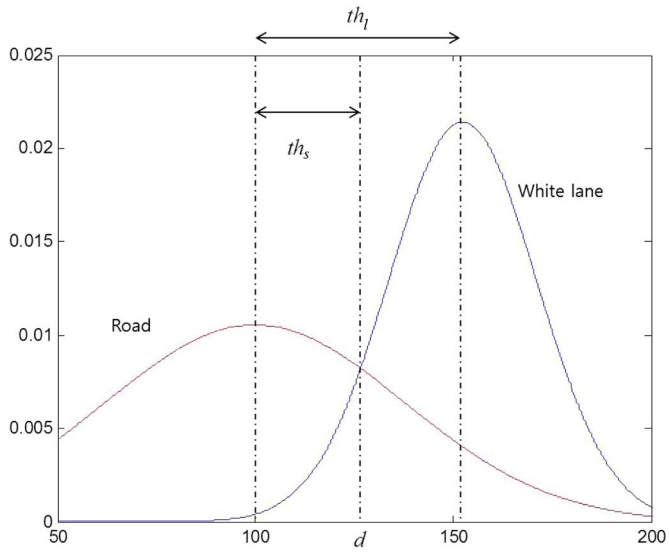

Fig. 7. Road and lane value distributions and Canny edge thresholds.

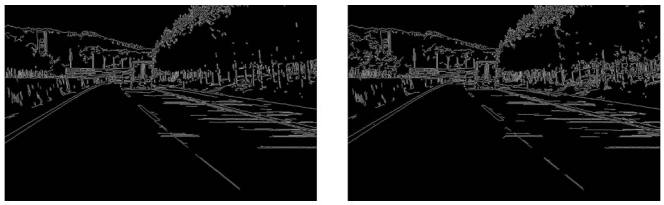

(a) (b)

Fig. 8. Canny edge detection results for (a) Fig. 5(a) and (b) Fig. 5(b).

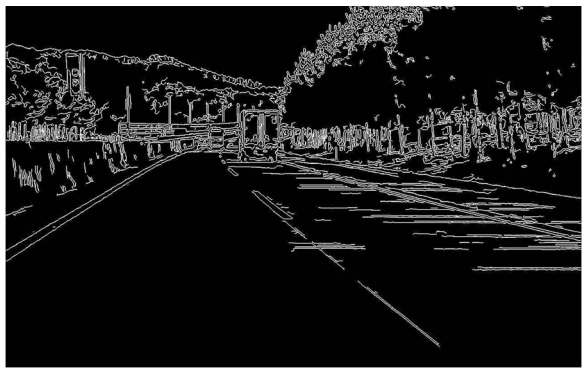

Fig. 9. Overall edge detection result of the proposed method.

threshold values to determine edges. Pixels with gradient values above the larger threshold th_l are selected as edges. On the other hand, pixels with values below the smaller threshold th_s are determined as nonedges. Pixels between the two thresholds are set as edge candidates and are classified as edges if there is a path from the pixel to an edge. Thus, two threshold values significantly affect the performance of edge detection. The adaptive threshold values for the Canny edge detector are required since the lane gradient in a converted image may vary with illumination. These adaptive thresholds are calculated from statistical characteristics of the road and lane class. Since RGB vectors of the road and lane are normally distributed [9] and the gradient-enhancing conversion is a kind of projection, the converted values of each class are also normally distributed. Distribution of the converted values of each class can be represented as follows:

$$p_c(\mathbf{w}\mathbf{x}^T) = \frac{1}{\sqrt{2\pi\sigma_c^2}} \exp\left\{\frac{(\mathbf{w}\mathbf{x}^T - \mathbf{m}_c)^2}{2\sigma_c^2}\right\} \qquad (13)$$

where c is a certain class, $\mathbf{m}_c$ is a mean of class c, $\mathbf{w}$ is a gradient-enhancing conversion vector between the lane class and the road class, and $\mathbf{w}\mathbf{x}^t$ is a gradient-enhancing converted value of $\mathbf{x}$ by $\mathbf{w}$. The distributions of the classes can be modeled without an additional process, since we calculate the means

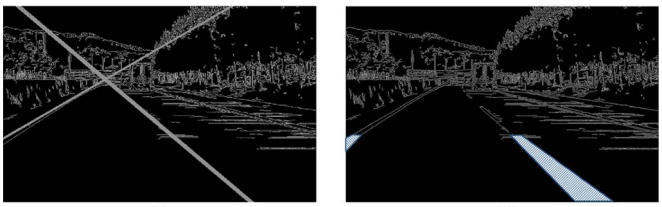

(a) (b)

Fig. 10. (a) Initial lane founded by HT. (b) Initial interesting region for extracting lane edges.

Fig. 11. Example of a curved-lane image.

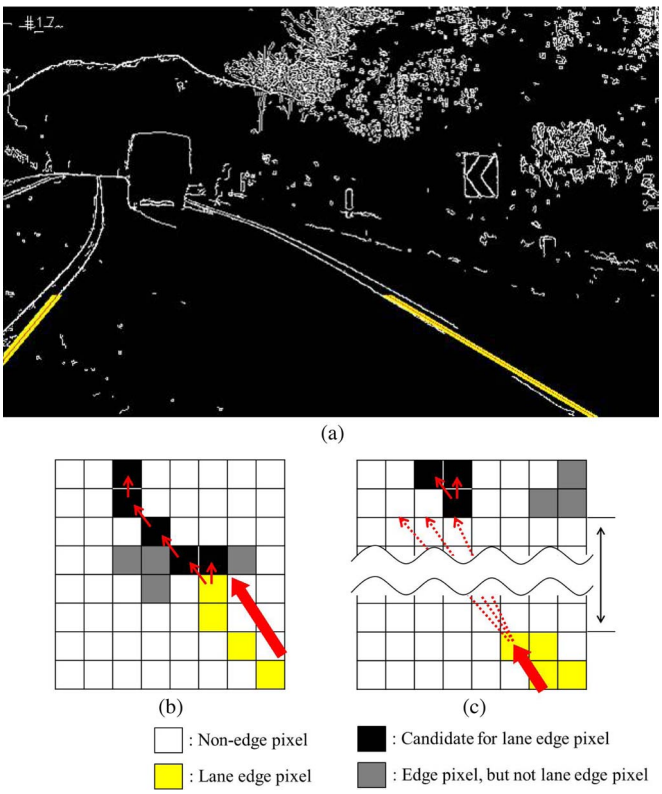

Fig. 12. Lane edge extraction. (a) Lane edges in the lower region. (b) Connected-lane case. (c) Dotted-lane case.

and variances of the classes in the previous gradient-enhancing conversion step. The large threshold value for the Canny edge detector is then a criterion for definite edges and is determined as follows:

$$th_l = |\mathbf{w} \cdot m^l - \mathbf{w} \cdot \mathbf{m}^r| \tag{14}$$

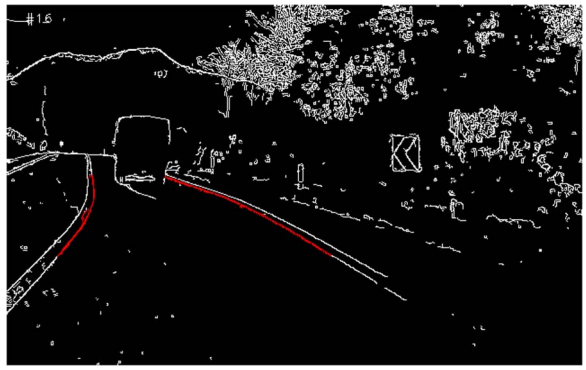

Fig. 13. Lane edges in the upper region of the road region.

TABLE II
ENVIRONMENT CONDITIONS FOR DRIVING DATABASE

Road Type	Time	Other Conditions
Highway	Day	Clear/Cloudy/Rainy
	Sunset/Sunrise	Clear/Cloudy, Lens flare
	Night	Clear/Rainy, Streetlamps, Car lamps
Route	Day	Clear/Cloudy/Rainy
	Sunset/Sunrise	Clear/Cloudy, Lens flare
	Night	Clear/Rainy, Streetlamps, Car lamps
Urban roads	Day	Clear/Cloudy/Rainy
	Sunset/Sunrise	Clear/Cloudy, Lens flare
	Night	Clear/Rainy, Streetlamps, Car lamps
Tunnel	N/A	White lamp/Yellow lamp

where th_l is a large threshold value for the Canny edge detector of the lane-gradient-enhanced image. A small threshold value for the Canny edge detector can be determined as follows:

$$th_s = \max\left(|\mathbf{w} \cdot \mathbf{m}^l - d|, |\mathbf{w} \cdot \mathbf{m}^r - d|\right) \tag{15}$$

where th_s is a smaller threshold value for the Canny edge of the gradient-enhanced image, and d is a value for which lane and road probabilities are equal. The meaning of threshold values is graphically represented in Fig. 7. Since the Canny edge detection algorithm is independently applied to each converted image, threshold values for the Canny edge detector are separately determined, and two edge maps are generated from one color image, as shown in Fig. 8. These maps are combined into one edge map by an OR operation, as shown in Fig. 9. In comparison with the previous method shown in Fig. 4, lane edges are more suitably detected, and noise is satisfactorily reduced. Thus, the lane can be more adequately detected with this edge map, as shown in Fig. 9.

After an edge map is generated, the HT is used for initial estimation of lane candidates. The HT changes the global pattern detection problem into an easier peak point detection problem. That is why the HT is widely used in lane detection algorithms. The process of accumulating votes for a possible line can be represented as follows [20]:

$$H(\rho, \theta) = \int \int I(u, v)\delta(\rho - u\cos\theta - v\sin\theta)dudv \tag{16}$$

where $H(\rho, \theta)$ is the number of votes for a line parameterized by ρ and θ, and $I(u, v)$ is a datum in the image space. The

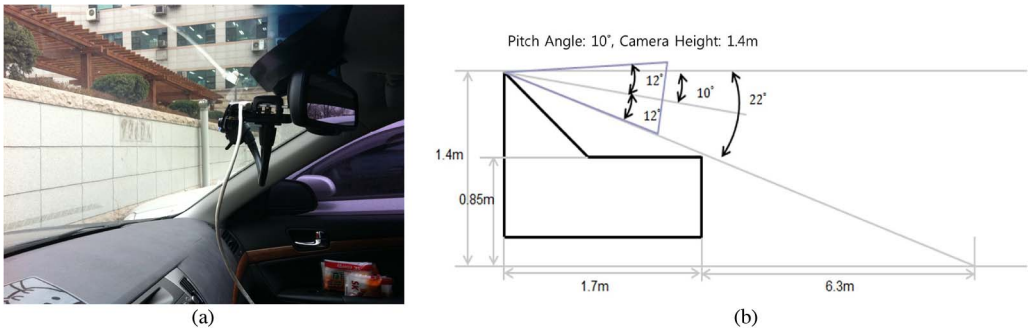

Fig. 14. Experimental setup. (a) In-vehicle vision sensor system. (b) Vision sensor setup configuration.

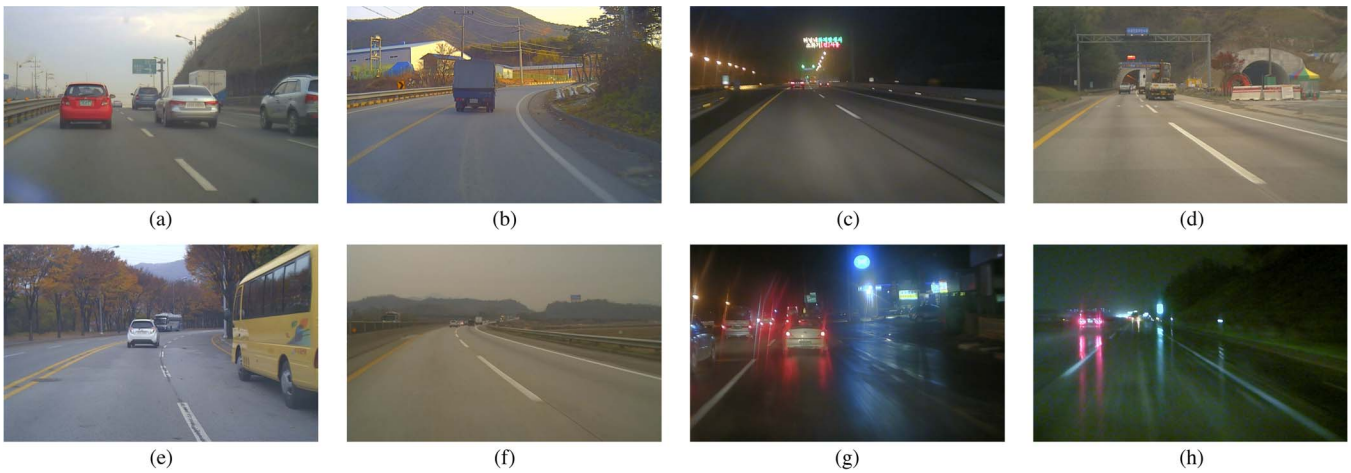

Fig. 15. Examples of database in various driving conditions. (a) Urban road in daylight with moderate traffic. (b) Prefectural road at sunset. (c) Highway at night with light traffic. (d) Highway tunnel. (e) Urban road in daylight. (f) Highway on a cloudy day. (g) Urban road on a rainy night with moderate traffic. (h) Highway on a rainy night.

HT-based algorithms generally assume that lanes are represented as lines. Fig. 10 shows the result of detecting lanes in Fig. 9 by HT. Since lanes in Fig. 11 are straight, HT seems to identify the correct lane. However, curved lanes are not represented as a line in an image, and HT cannot follow curved lanes, as shown in Fig. 11. Nevertheless, the method can be used as an initial estimation for lane detection, since lanes still can be viewed as lines at the bottom of the image. We select the initial interesting region for extracting lane edges near the initial lines founded by HT, as shown in Fig. 10(b).

Lane edges are found by using the edge direction constraint in the interesting region. The slope curved lane is changed into a different value from the slope of the HT line in the upper region of the road region, as shown in Fig. 11. Edges in the initial interesting region are collected as lane edges if they have a similar slope to the HT line, as shown in Fig. 12(a). For the upper region, we search the upper region along the tangential direction of lane edges in the lower region, since lane edges are generally connected, as shown in Fig. 12(b). In dotted- or removed-lane cases, there can be no edge component among the upper neighborhoods. In these cases, we pass the rows along the tangential direction of the previous lane edges until meeting a candidate for the lane edge, as shown in Fig. 12(c). Fig. 13 shows the lane edge extraction result for the upper region in Fig. 11.

Finally, we generate fitted curved lanes using lane edges. Curve fitting in the lane detection algorithm is usually used to represent curved lanes. Curved lanes are usually constructed using a clothoid curve model, which is complex to model. Thus, many algorithms use an approximated clothoid model. Kim [6] adopted a polynomial curve (including a quadratic curve and a cubic curve) to characterize the geometric road model. Zhow *et al.* [15] generated several candidates of projection of the 2-D lane geometric model in road plane coordinates and chose the best fitted candidate. However, the given methods to represent curved lanes are complex. Since most curved lanes are approximately represented by a constant curvature model, we use the quadratic curve model, which is less complex than the others. Thus

$$y = \frac{1}{2}c_0x^2 + mx + b \tag{17}$$

where x and y are coordinate values, c_0 is the curvature of the lane, m is the slope, and b is the offset of the lane. Since lanes in the camera coordinate system are represented by a projective transformation of the quadratic curve model, the model should be modified to estimate the lane model in an image. We use a model that is combined with a straight line and quadratic curve to approximate the projection lane model. Line parameters are

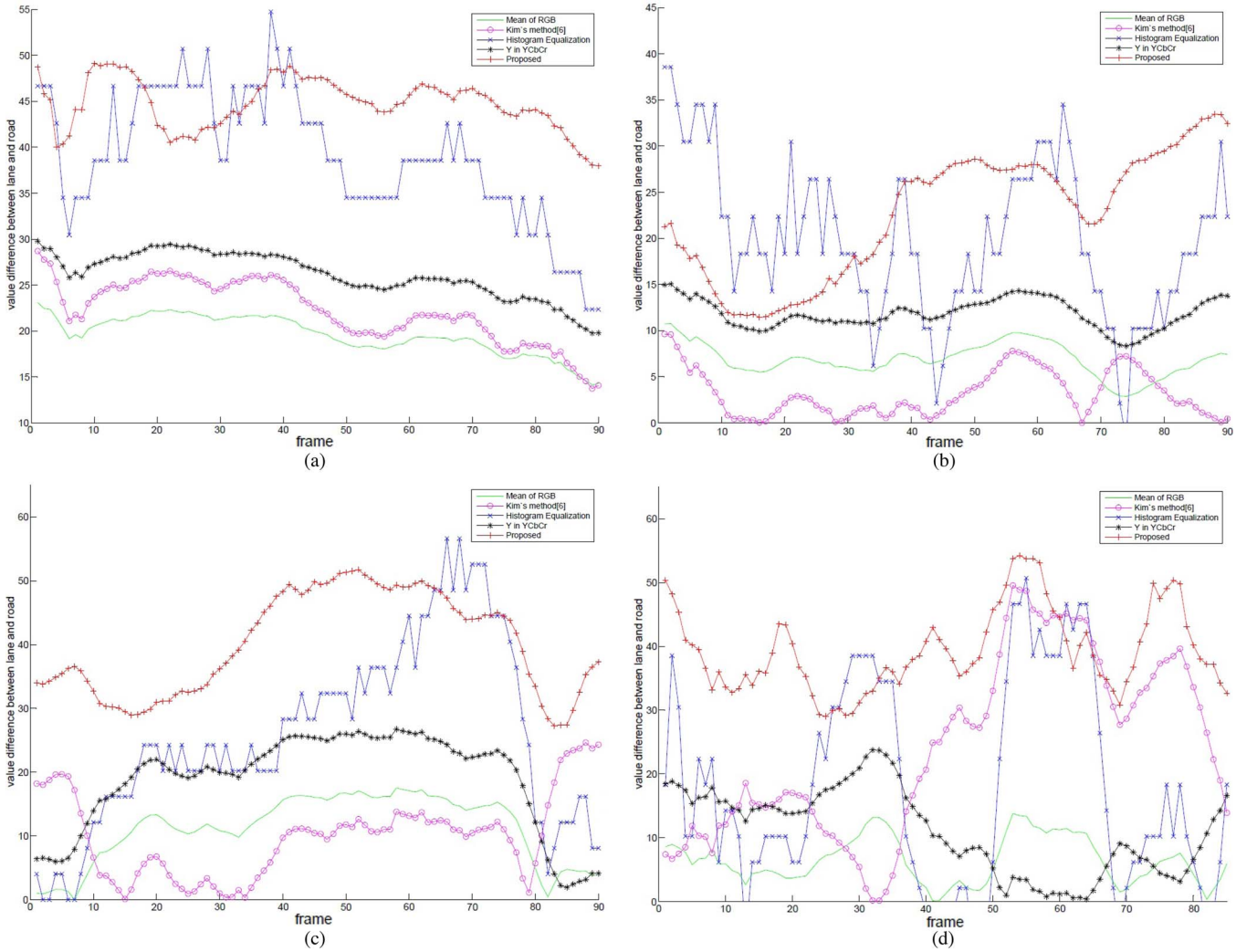

Fig. 16. Yellow-lane gradients in converted images consecutive sequences in Fig. 15(a)–(d).

derived from the curve parameters since the lane model is differentiable and continuous. Thus

$$y = \begin{cases} \frac{1}{2}c_0x^2 + mx + b, & x < x_0 \\ m'x + b', & x \geq x_0 \end{cases} \quad (18)$$

$$m' = \frac{d}{dx}\left(\frac{1}{2}c_0x^2 + mx + b\right)|_{x=x_0}, b' = b - \frac{1}{2}c_0x_0^2. \quad (19)$$

Three parameters of the quadratic curve are needed to estimate the lane model. The least squares method is used to find the parameters of a quadratic curve. Thus

$$SSD(c_0, m, b) = \sum_{x>x_0}\left(y_i - \left(\frac{1}{2}c_0x^2 + mx + b\right)\right)^2. \quad (20)$$

Training data for the next frame are updated based on lane detection results in the current frame. First, we select the interesting regions near the detected lanes. The new training data of class c, i.e., X_c^{t-1}, are collected based on the statistical characteristics of the training data for the frame at $t-1$, i.e., T_c^{t-1}. The Mahalanobis distance is used to measure the similarity between T_c^{t-1} and the frame at time $t-1$. Thus

$$MD_c(\mathbf{x}) = \sqrt{(\mathbf{x} - \mathbf{m_c})^T S_c^{-1}(\mathbf{x} - \mathbf{m_c})} \quad (21)$$

where $\mathbf{x}$ is an RGB vector of a pixel in the frame at $t-1$, $\mathbf{m_c}$ is a mean vector of class c, S_c is a covariance matrix of class c, and MD_c is the Mahalanobis distance between $\mathbf{x}$ and $\mathbf{m_c}$. If $MD_c(\mathbf{x})$ is less than a certain value, $\mathbf{x}$ is chosen as the new training data of class c.

For the initial frame of an image sequence, we manually crop patches of lane and road regions and use them as initial training data. Training data for other frames are then updated for adapting illumination changes.

IV. Experimental Result

A. Database Construction

The video database in various environmental conditions is needed to evaluate vision-based ADAS. Since the performance of a vision-based algorithm varies according to illumination changes, we consider illumination conditions for constructing the video database. Illumination changes in road environments may include natural and artificial light changes. Natural light changes are caused by time and weather, and artificial light changes are caused by the characteristics of streetlamps and vehicle lamps. The road type is another important factor in developing ADAS. Fast vehicles, straight roads, and clear

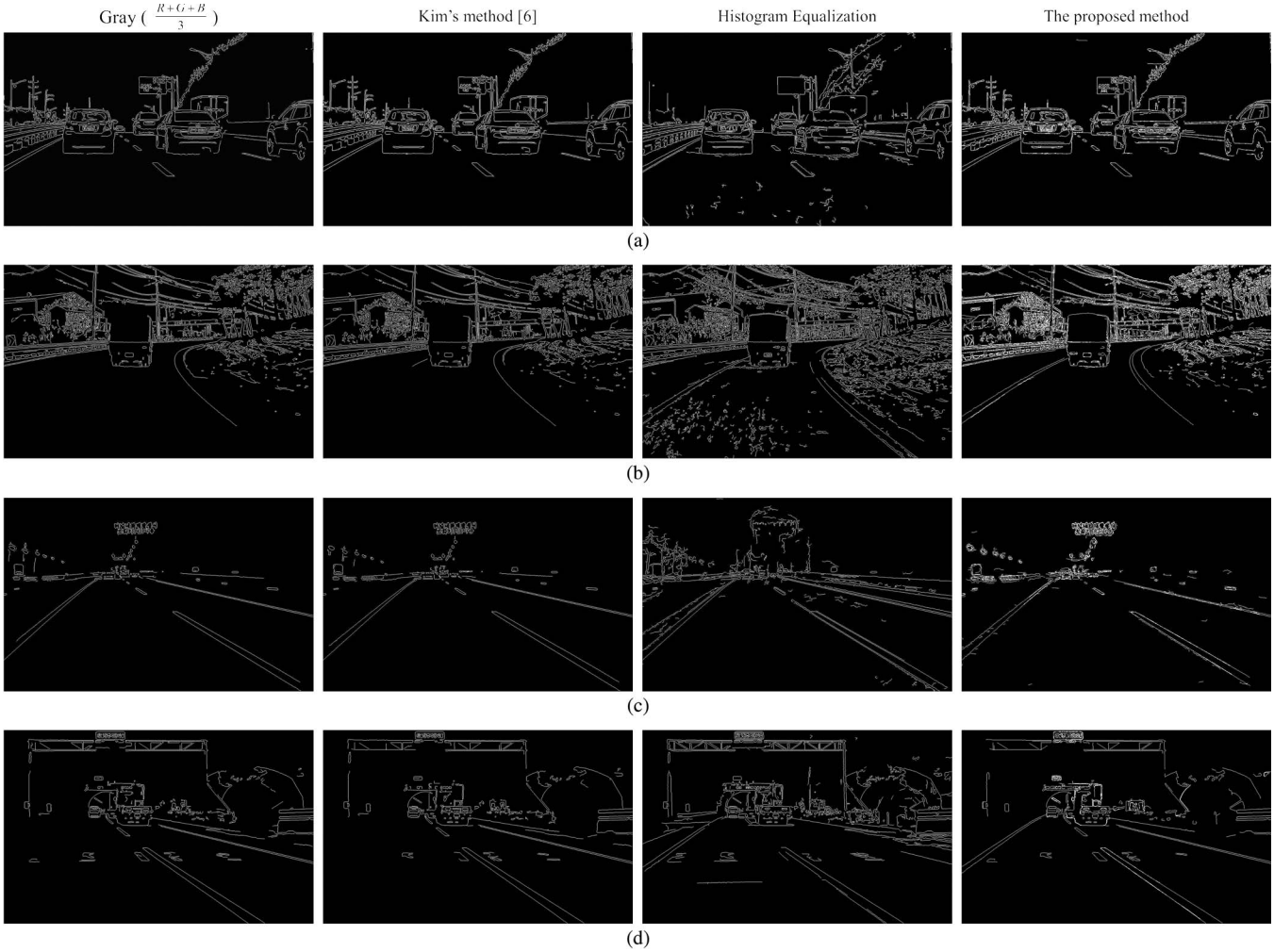

Fig. 17. Canny edge detection results for (a) Fig. 15(a), (b) Fig. 15(b), (c) Fig. 15(c), and (d) Fig. 15(d) ($th_s = 60$, $th_l = 100$).

lane marks are features of normal highways. On the other hand, routes and urban roads have many curves, blurred lane markings, and slower vehicles. Thus, we created driving scenarios considering these factors, as shown in Table II. We used an OV10630 image sensor, which provides 1280 $\times$ 800 resolution at 15 frames per second. The sensor is mounted behind the rear-view mirror, as shown in Fig. 14(a). The camera configuration is shown in Fig. 14(b). For two months, we constructed the database in downtown and urban roads of Korea. Since our database includes various situations such as traffic, pedestrians, and obstacles, it can be used to develop and evaluate various vision-based ADAS algorithms and lane detection algorithms. Fig. 15 shows some of the images in our database.

B. Gradient-Enhancing Conversion Results

We applied the gradient-enhancing conversion method to our database. We compared gradient values at lanes with the results of different methods to confirm improvements of the gradient at lanes. White-lane gradients are sufficiently large in the converted image of the conventional methods, and in the proposed method, yellow-lane gradients are not. Fig. 16 shows the yellow-lane gradient in the converted images of consecutive frames. The proposed method outperformed other methods in most cases, as shown in Fig. 16. Yellow-lane gradients increase by more than double in conventional gray-level images. Although the conventional methods produce lane gradients that are larger or similar to those of the proposed method in several cases, they do not produce stable results in illumination changes. Compared with other methods, the proposed method produces larger lane gradients under various illumination conditions.

Gradient enhancement affects edge detection performance. We convert the images in Fig. 15(a)–(d) using conventional methods and the proposed method. We then apply the Canny edge detector with the same threshold values to the converted images. Fig. 17 shows edge detection results of the converted images. Results of the histogram equalization-based method adequately detected lane edges in most cases, but many unwanted edges were also included. Since histogram equalization enhances the contrast of an image, it enhances all unwanted and lane gradients. The method of Kim [6] and the gray channel-based method produce clear lane edge detection results, such as in Fig. 17(a) and (c). However, they do not show stable performance for lane edge detection, as shown in Fig. 17(b) and (d). The results of the proposed method have lane edges and do not contain unwanted edges in all cases because the proposed

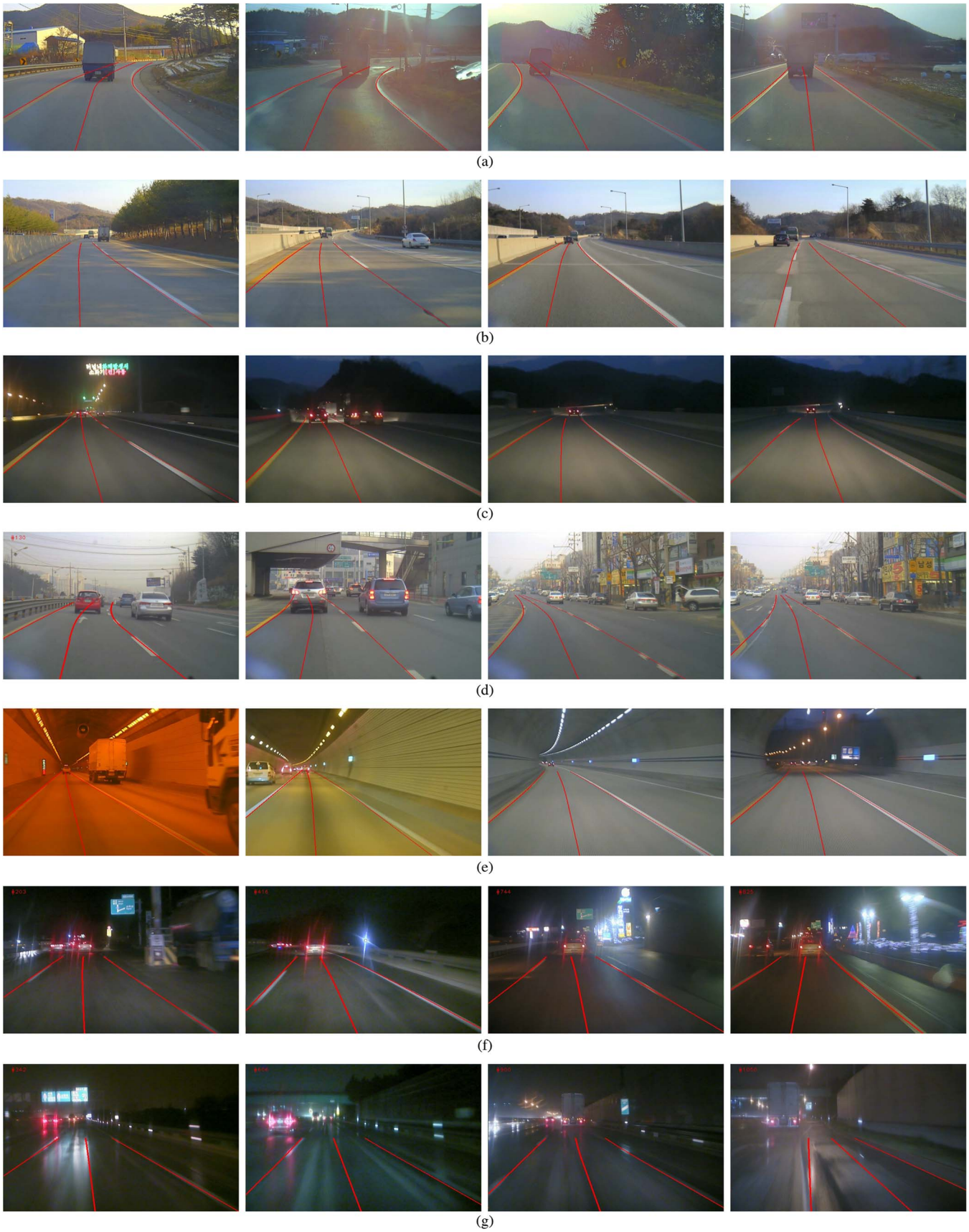

Fig. 18. Lane detection results under various driving conditions.

(a) (b) (c) (d)

Fig. 19. Examples for false-detection results. (a) Wrong bending direction. (b) Fail to detect curved lane. (c) Not on lane marks. (d) Not on lane marks and wrong bending direction.

TABLE III
LANE DETECTION RATE OF THE PROPOSED ALGORITHM IN VARIOUS ENVIRONMENTS

Data Set	Route-Sunset	Highway-Day	Highway-Night	Urban-Day	Night-Lamp	Tunnel	Rainy	Total
Total Frames	1080	609	881	1574	735	2157	997	8033
Detected Frames	1022	576	876	1498	684	2127	959	7742
Detection Rate(%)	94.63	94.58	99.43	95.17	93.19	98.61	96.19	96.37

method causes the converted images to have reducing gradients in homogeneous regions and enhancing gradients in interesting regions. That is, lane detection is much easier in the results of the proposed edge detection method.

C. Lane Detection Results

We simulate the lane detection algorithm with several databases. More than 8000 frames in various illumination conditions from the databases are used to show the illumination robustness of the proposed lane detection algorithm. To evaluate the proposed lane detection algorithm, we measure the detection rate. We manually count the number of correct detection frames and determine that detection frames are correct if detection lanes are on real lane markings and their bending directions are correct, as shown in Fig. 18. Fig. 19 shows examples of false-detection frames. In most conditions, detection rates are near 95%, and detection rates remain greater than 93%, even under poor illumination conditions. The average detection rate is 96.37%, as summarized in Table III. The performance of the proposed lane detection algorithm is not largely affected by illumination changes. In addition, we simulate other lane detection methods [21], [22] to compare the lane detection rate with the proposed method. Both compared algorithms are based on a kind of gradient features and inverse perspective mapping (IPM). The lane detection rate of each method is shown in Table IV. The detection rate of the method of Aly is about 72% for our database since it does not consider environment changes and curved lanes. The method of Borkar *et al.*, which is based on adaptive threshold, shows better performance than that of Aly, but it is still around 81%. IPM-based lane detection methods are easily false detection on a forward vehicle since IPM transform a forward vehicle to be similar to lane component. The proposed method shows the best performance, and the lane detection rate of every method is improved by over 10% when they use the gradient-enhanced image. The improvement is because the comparison methods also use a kind of gradient features. It means that the proposed gradient-enhancing method can be applied to other lane detection methods based on gradient features to improve environment robustness.

TABLE IV
LANE DETECTION RATE OF COMPARISON

	Detection Rate using Gray Image	Detection Rate using Enhanced Image
Aly's method [21]	72.94%	89.41%
Borkar's method [22]	81.53%	92.71%
Proposed Method	85.32%	96.37%

The overall process requires approximately 50 ms in each frame. This means that the lane detection algorithm can be used for real-time applications.

V. CONCLUSION

This paper has proposed gradient-enhancing conversion and an illumination-robust lane detection algorithm. Gradient-enhancing conversion produces a color image of an intensity image that has maximized gradients at the lanes. This process provides strong edges to the lane boundary in various illumination conditions so that the proposed lane detection algorithm is robust to illumination changes. To verify the performance of the proposed algorithm, we compare the lane gradients and show lane detection results under various illumination conditions in the experimental section. White-lane gradients are slightly better, and yellow-lane gradients are improved by more than double compared with those in conventional methods. The lane detection algorithm based on the proposed gradient-enhancing conversion method shows a detection rate that is, on average, greater than 96% under various illumination conditions, and the performance of the proposed lane detection method continues to be greater than 93% under poor conditions. In addition, the gradient-enhancing conversion method does not involve high computational complexity. The proposed lane detection algorithm takes 50 ms per frame and, thus, can be used for real-time applications. Moreover, the proposed gradient-enhanced image can improve the performance of other lane detection algorithms based on gradient features. However, the conversion method

does not work well in extremely different multi-illumination conditions, such as water reflection in heavy rainfall at night, because we assume that one scene does not have multiple illuminations. To overcome this limitation, we will establish another imaging model that works in problematic conditions and apply the lane detection algorithm.

REFERENCES

[1] J. C. McCall and M. M. Trivedi, "Video based lane estimation and tracking for driver assistance: Survey, system and evaluation," *IEEE Trans. Intell. Transp. Syst.*, vol. 7, no. 1, pp. 20–37, Mar. 2006.

[2] Y. He, H. Wang, and B. Zhang, "Color-based road detection in urban traffic scenes," *IEEE Trans. Intell. Transp. Syst.*, vol. 5, no. 4, pp. 309–318, Dec. 2004.

[3] Y. U. Yim and S.-Y. Oh, "Three-Feature based Automatic Lane Detection Algorithm (TFALDA) for autonomous driving," *IEEE Trans. Intell. Transp. Syst.*, vol. 4, no. 4, pp. 219–225, Dec. 2003.

[4] Y. Wang, N. Dahnoun, and A. Achim, "A novel system for robust lane detection and tracking," *Signal Process.*, vol. 92, no. 2, pp. 319–334, Feb. 2012.

[5] R. X. Yong Zhou, X. Hu, and Q. Ye, "A robust lane detection and tracking method based on computer vision," *Meas. Sci. Technol.*, vol. 17, no. 4, pp. 736–745, Apr. 2006.

[6] Z. Kim, "Robust lane detection and tracking in challenging scenarios," *IEEE Trans. Intell. Transp. Syst.*, vol. 9, no. 1, pp. 16–26, Mar. 2008.

[7] N. Apostoloff and A. Zelinsky, "Robust vision based lane tracking using multiple cues and particle filtering," in *Proc. IEEE IV Symp.*, San Diego, CA, USA, Jun. 2003, pp. 558–563.

[8] T.-Y. Sun, S.-J. Tsai, and V. Chan, "HSI color model based lane-marking detection," in *Proc. IEEE ITSC*, Toronto, ON, Canada, Sep. 2006, pp. 1168–1172.

[9] H.-Y. Cheng, B.-S. Jeng, P.-T. Tseng, and K.-C. Fan, "Lane detection with moving vehicles in the traffics scenes," *IEEE Trans. Intell. Transp. Syst.*, vol. 7, no. 4, pp. 571–582, Dec. 2006.

[10] J. Wang, Y. Wu, Z. Liang, and Y. Xi, "Lane detection and tracking using a layered approach," in *Proc. IEEE Int. Conf. Inf. Autom.*, Harbin, China, Jun. 2010, pp. 1735–1740.

[11] J.-G. Wang, C.-J. Lin, and S.-M. Chen, "Applying fuzzy method to vision-based lane detection," *Exp. Syst. Appl.*, vol. 37, no. 1, pp. 113–126, Jan. 2010.

[12] M. Jacob and M. Unser, "Design of steerable filters for feature detection using canny-like criteria," *IEEE Trans. Pattern Anal. Mach. Intell.*, vol. 26, no. 8, pp. 1007–1019, Aug. 2004.

[13] M. Meuter, S. Muller-Schneiders, A. Mika, S. Hold, C. Nunn, and A. Kummert, "A novel approach to lane detection and tracking," in *Proc. IEEE ITSC*, St. Louis, MO, USA, Oct. 2009, pp. 582–587.

[14] B. Yu and W. Zhang, "A robust approach of lane detection based on machine vision," in *Proc. IITA Int. Conf. CASE*, Zhangjiajie, China, Jul. 2009, pp. 195–198.

[15] S. Zhow, J. Xi, J. Gong, G. Xiong, and H. Chen, "A novel lane detection based on geometrical model and Gabor filter," in *Proc. IEEE IV Symp.*, San Diego, CA, USA, Jun. 2010, pp. 59–64.

[16] M. Tian, F. Liu, W. Zhu, and C. Xu, "Vision based lane detection for active security in intelligent vehicle," in *Proc. IEEE ICVES*, Dec. 2006, pp. 507–511.

[17] Q.-B. Truong and B.-R. Lee, "New lane detection algorithm for autonomous vehicles using computer vision," in *Proc. Int. Conf. Control, Autom. Syst.*, Seoul, Korea, Oct. 2008, pp. 1208–1213.

[18] J. Wang, Y. Wu, Z. Liang, and Y. Xi, "Lane detection based on random Hough transform on region of interesting," in *Proc. IEEE ICIA*, Jun. 2010, pp. 1735–1740.

[19] U. Yang and K. Sohn, "Image-based color temperature estimation for color constancy," *IET Electron. Lett.*, vol. 47, no. 5, pp. 322–324, Mar. 2011.

[20] J. B. McDonald, "Application of the Hough transform to lane detection and following on high speed roads," in *Proc. Irish Signals Syst. Conf.—Motorway Driving Scenarios*, Maynooth, Ireland, 2001.

[21] M. Aly, "Real time detection of lane markers in urban streets," in *Proc. IEEE Intell. Veh. Symp.*, Jun. 2008, pp. 7–12.

[22] A. Borkar, M. Hayes, and M. Smith, "A novel lane detection system with efficient ground truth generation," *IEEE Trans. Intell. Transp. Syst.*, vol. 13, no. 1, pp. 365–374, Mar. 2012.

Hunjae Yoo received the B.S. degree from Yonsei University, Seoul, Korea, in 2009, where he is currently working toward the joint M.S./Ph.D. degree in electronic and electrical engineering.

His research interests include computer vision, pattern recognition, and color image processing.

Ukil Yang received the B.S., M.S., and Ph.D. degrees in electronic and electrical engineering from Yonsei University, Seoul, Korea, in 2002, 2005, and 2011, respectively.

His research interests include pattern recognition and color image processing.

Kwanghoon Sohn (SM'12) received the B.E. degree in electronics engineering from Yonsei University, Seoul, Korea, in 1983; the M.S.E.E. degree in electrical engineering from the University of Minnesota, Minneapolis, MN, USA, in 1985; and the Ph.D. degree in electrical and computer engineering from North Carolina State University, Raleigh, NC, USA, in 1992.

From 1992 to 1993, he was a senior member of the research staff with the Satellite Communication Division, Electronics and Telecommunications Research Institute, Daejeon, Korea. He was also a Postdoctoral Fellow with the Magnetic Resonance Imaging Center, Georgetown University Medical Center, Washington, DC, USA. From 2002 to 2003, he was a Visiting Professor with Nanyang Technological University, Singapore. He is currently a Professor with the School of Electrical and Electronic Engineering, Yonsei University. His research interests include 3-D image processing, computer vision, and image communication.

Dr. Sohn is a member of the Society of Photo-Optical Instrumentation Engineers.